• Clinical Research •

A novel mutation of *CYP4V2* gene associated with Bietti crystalline dystrophy complicated by choroidal neovascularization

Xin-Yao Han, Lin-Qi Zhang, Ji-Yang Tang, Lyu-Zhen Huang, Ran Tang, Jin-Feng Qu

Department of Ophthalmology, Peking University People's Hospital; Eye Diseases and Optometry Institute; Beijing Key Laboratory of Diagnosis and Therapy of Retinal and Choroid Diseases, College of Optometry, Peking University Health Science Center, Beijing 100044, China

Correspondence to: Jin-Feng Qu. Department of Ophthalmology, Peking University People's Hospital, No.11 S Ave of Xizhimen, Xicheng District, Beijing 100044, China. qujinfeng_pkuph@126.com

Received: 2021-11-03 Accepted: 2022-01-27

Abstract

● **AIM:** To investigate the clinical characteristics and genetic features of a Bietti crystalline dystrophy (BCD) proband in a Chinese family.

● **METHODS:** A Chinese female diagnosed with BCD complicated by bilateral choroidal neovascularization (CNV) and her parents underwent complete ophthalmic examinations, including fundus autofluorescence (AF), fundus photography (FP), fundus fluorescein angiography (FFA), visual field testing, full-field electroretinography (ERG), optical coherence tomography (OCT) and optical coherence tomography angiography (OCTA). The sequencing of the *CYP4V2* gene was performed to the whole family.

● **RESULTS:** Bilateral tiny glittering crystal-like deposits and differing extent of atrophy of the retinal pigment epithelium (RPE) were found in the posterior pole of her fundus. The diffuse hypo-fluorescence shown on AF images and window defects shown on FFA both indicated the atrophy of the RPE and choriocapillaris. OCT showed the thinning of the RPE and choriocapillaris layer, ellipsoid zone (EZ) band defect and CNV in both eyes. OCTA images proofed bilateral type 2 CNV. The visual field test showed central and paracentral scotoma. ERG showed a slightly decreased b-wave in scotopic ERG. Gene sequencing identified three mutations of the *CYP4V2* gene, c.802_807del, c.810delT, and c.1388G>A. The mutation c.1388G>A was a novel substitution mutation.

● **CONCLUSION:** The novel mutation c.1388G>A may be a possible cause that could induce the clinical phenotype of BCD.

● **KEYWORDS:** Bietti crystalline dystrophy; retinal degeneration; *CYP4V2* gene; choroidal neovascularization

DOI:10.18240/ijo.2022.06.11

Citation: Han XY, Zhang LQ, Tang JY, Huang LZ, Tang R, Qu JF. A novel mutation of *CYP4V2* gene associated with Bietti crystalline dystrophy complicated by choroidal neovascularization. *Int J Ophthalmol* 2022;15(6):940-946

INTRODUCTION

Bietti crystalline dystrophy (BCD, MIM210370), first reported by Bietti in 1937, is an autosomal recessive disorder of chorioretinal degeneration. It is characterized by tiny sparkling yellowish crystals in the posterior pole, retinal pigment epithelium (RPE) atrophy, and choroidal sclerosis[1]. Crystals in the corneal limbus and circulating lymphocytes have also been reported in some cases[2-3]. Although BCD is a rare form of non-syndromic retinitis pigmentosa (RP), it is relatively common in China and Japan. According to Hu's[4] epidemiological survey in 1982, the prevalence rate of BCD in China was 0.5%, though some researchers think the prevalence rate is underestimated. There are some differences between BCD and other autosomal recessive RP in clinical characteristics and imaging performances, which deserving our attention.

BCD is caused by mutations of the *CYP4V2* gene (Gene ID 285440, OMIM 210370), with multiple genotypic and phenotypic variations[5]. The *CYP4V2* gene is located on chromosome 4 (4q35), comprising of 11 exons and encoding a protein of 525 amino acids, a member of the cytochrome P450 protein family[6]. The protein serves as an enzyme in fatty acids metabolism.

Early symptoms of BCD are similar to other autosomal recessive RP, including gradual reduction of visual acuity, paracentral scotomas, visual field constriction, night blindness, and color vision defects. Severe cases may progress to legal blindness at late stages about 50-60s[7]. Phenotype polymorphism has been observed, sometimes patients from the same family with the same mutations can have different phenotypes.

Choroidal neovascularization (CNV) is associated with RPE and Bruch's membrane breaches. It is rare in hereditary retinal degeneration, except for a few conditions, including BCD. As a complication of BCD, it could be a severe threat to vision. There has been no previous report of any mutations associated with CNV in BCD.

The discoveries of the *CYP4V2* mutations reported before allowed ophthalmologists to test the correlation between genotype and phenotype. In this study, we report the results of clinical examinations of a Chinese BCD patient and genetic analyses of the *CYP4V2* gene of her family. We identified three *CYP4V2* mutations in mutation screening of the *CYP4V2* gene, one of which was novel.

SUBJECTS AND METHODS

Ethical Approval This study was conducted at the Department of Ophthalmology, Peking University People's Hospital, Beijing, China. The study was performed under the Declaration of Helsinki tenets after approval by Ethics Committee of Peking University People's Hospital (2020PHB250-1). Informed consent was obtained from all individuals included in the study.

A 30-year-old female (the daughter of the family) with suspected BCD and her family all underwent ophthalmologic examinations, including best-corrected visual acuity (BCVA), intraocular pressure (IOP), slit-lamp examination, dilated fundoscopy in order to exclude other ocular diseases. The proband patient underwent comprehensive ophthalmic examinations, including fundus autofluorescence (AF), fundus photography (FP), fundus fluorescein angiography (FFA), Ganzfeld full-field electroretinograms (ERGs), Humphrey visual field, optical coherence tomography (OCT), and optical coherence tomography angiography (OCTA). Clinical diagnosis was made based on tiny sparkling yellowish crystals in the posterior pole, and the atrophy of RPE and choriocapillaris.

The genomic DNA of four members in this family was extracted from their peripheral blood with a High Pure PCR Template Preparation Kit (Roche, Basel, CH, USA). DNA fragments were enriched by solution-based hybridization capture, then sequenced on the Illumina Miseq platform (Illumina, San Diego, CA, USA) with the 2×300-bp paired-end read module. The hybridization capture procedure was performed with SureSelect Library Prep Kit (Agilent, Santa Clara, CA, USA). Deep intronic sequences were not targeted to avoid decreasing the mean sequence coverage. DNA was sheared *via* sonication with Diangenode Bioruptor® Plus and hybridized with biotinylated RNA oligonucleotide baits. Captured fragments were removed by using streptavidin-coated magnetic beads (Dynabeads® MyOne™ Streptavidin T1, Thermo Fisher Scientific) and then eluted. The enriched fragment library was amplified by PCR using primers specific to the linked Illumina adaptors. The resulting libraries were quantified using Q-PCR before proceeding to the Illumina Miseq platform. All samples were sequenced together and 6-bp index sequences (Illumina) were used to distinguish samples. Raw reads from samples were sorted by index sequences after sequencing. Adapter sequences were trimmed by Cutadapt. SolexaQA was used to remove low-quality bases. Clean Reads were aligned to the human reference genome (hg19) with Burrows-Wheeler Aligner (BWA; v.0.7.11). Realignment around known indel sites and Base Quality Score Recalibration (BQSR) were performed by GATK (v.3.3). Human Gene Mutation Database, dbSNP138, 1000 Genome project, ClinicVar, and Exome Sequencing Project were used to screen variants. To detect copy number variants, the sequencing depth of each region covered by probes was calculated according to the alignment files. Functional effect prediction was evaluated by Provean, PolyPhen-2, and Mutation Taster. After candidate causative mutations were determined, the samples were sequenced by Sanger sequencing to verify the mutations and performed with genotype-phenotype co-segregation analysis.

RESULTS

The proband, a 30-year-old female, presented with decreased vision with metamorphopsia in her right eye for half a year. The patient received bilateral refractive surgery in 2013 before which she had myopia of -6.00 diopter of spherical power (DS) in both eyes. The patient's medical records showed she used to attain normal visual acuity in both eyes post refractive surgery. There was no other history of diagnosed eye conditions.

Her BCVA was 20/100 (0.20 logMAR) of right eye, and 20/25 (0.8 logMAR) of left eye. Her IOP was normal. Slit lamp examination showed no remarkable anterior segment findings. No crystalline deposits in the cornea and corneal limbus have been observed. Fundus examination showed glittering yellowish crystalline deposits in the posterior pole with diffuse RPE atrophy (Figure 1). AF images showed diffuse hypo-fluorescence interspersed with hyper-fluorescence scatters in and beyond the posterior pole (Figure 1). OCT images showed thinning and loss of the RPE layer, interruption and loss of the interdigitation zone (IZ) and ellipsoid zone (EZ). Residual EZ layer and RPE can be observed at the fovea. Outer retinal tubulations (ORTs) and atrophy of the choriocapillaris has been observed. OCT and OCTA also demonstrated that active type 2 choroidal neovascular membrane in both eyes (Figure 2). The FFA images showed widespread window defects with multiple scattered hypo-fluorescent spots and leakage in the fovea indicating active CNV in both eyes (Figure 3). Visual field revealed central scotoma and paracentral scotoma in both eyes (Figure 4). Full-field ERG showed a slightly decreased

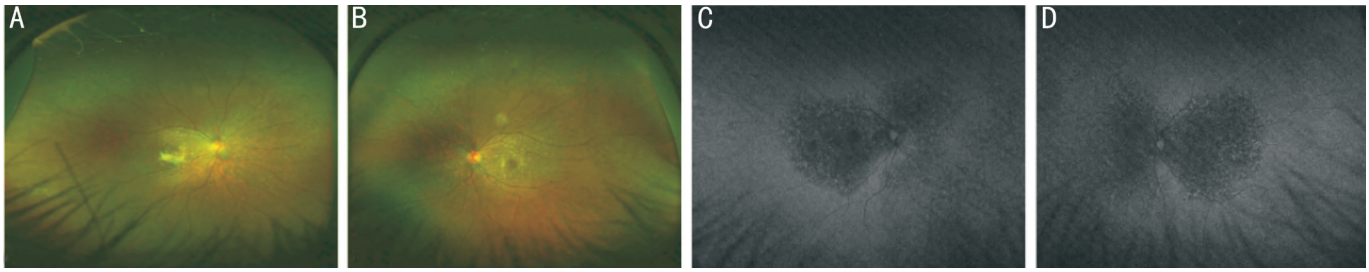

Figure 1 Color fundus photographs and fundus autofluorescence (AF) images of the patient A, B: Fundus examination showed numerous tiny glittering crystalline deposits at the posterior pole (more concentrated around the macula) and retinal pigment epithelium (RPE) atrophy (A: right eye, B: left eye); C, D: AF images showed diffuse hypo-fluorescence interspersed with hyper-fluorescence scatters in and beyond the posterior pole. Small confluent hypo-fluorescent patches in both eyes' posterior poles indicating the atrophy of RPE (C: right eye, D: left eye).

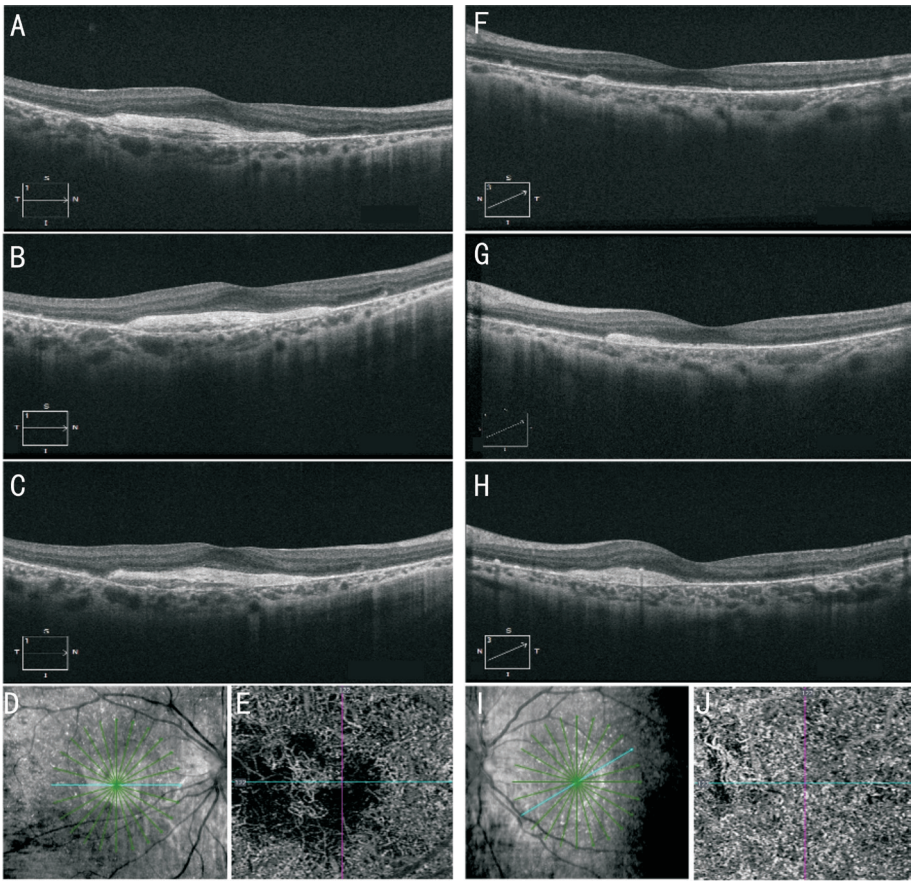

Figure 2 Optical coherence tomography (OCT) and optical coherence tomography angiography (OCTA) images of the patient A-D, F-I: OCT images showed thinning of the RPE layer, interruption and loss of the interdigitation zone (IZ) and ellipsoid zone (EZ), residual EZ layer and RPE layer at the fovea, outer retinal tubulations (ORTs) and atrophy of the choriocapillaris (A-D: right eye, F-I: left eye). OCT also demonstrated that active type 2 choroidal neovascular membrane in both eyes. E, J: OCTA images also confirmed neovascularization in both eyes (E: right eye, J: left eye).

b-wave amplitude in scotopic ERG (Figure 5). Ophthalmic examinations of other family members showed no remarkable findings.

Compared with the complete sequence of the coding and adjacent intron regions of the *CYP4V2* gene, three heterozygous mutations were found in the proband patient: c.802_807del (p.V268_I269del), c.810delT (p.E271Nfs*5) and c.1388G>A (p.G463D). The father had c.802_807del mutation and c.810delT mutation. The mother had c.1388G>A mutation. The brother had no mutation (Table 1).

The substitution mutation c.1388G>A is a novel mutation never been reported in the Human Gene Mutation Database (HGMD) and predicted to be pathogenic. The score values of the novel mutation based on three bioinformatics tools are high, suggesting that the mutation causes protein dysfunction and is harmful to the patients. The c.810delT and c.802_807del are deletion mutations that have been reported in BCD patients as pathogenic mutations[8].

Table 1 CYP4V2 gene mutations of the proband and her family

Nucleotide	Amino acid	Computational prediction			Family member	Genotype
		Provean	Polyphen-2	Mutation taster		
c.802_807del	p.V268_I269del	Not available	Not available	Polymorphism	Proband	Heterozygous
					Brother	No mutation
					Father	Heterozygous
					Mother	No mutation
c.810delT	p.E271Nfs*5	Not available	Not available	Disease causing	Proband	Heterozygous
					Brother	No mutation
					Father	Heterozygous
					Mother	No mutation
c.1388G>A	p.G463D	Deleterious	Probably damaging	Disease causing	Proband	Heterozygous
					Brother	No mutation
					Father	No mutation
					Mother	Heterozygous

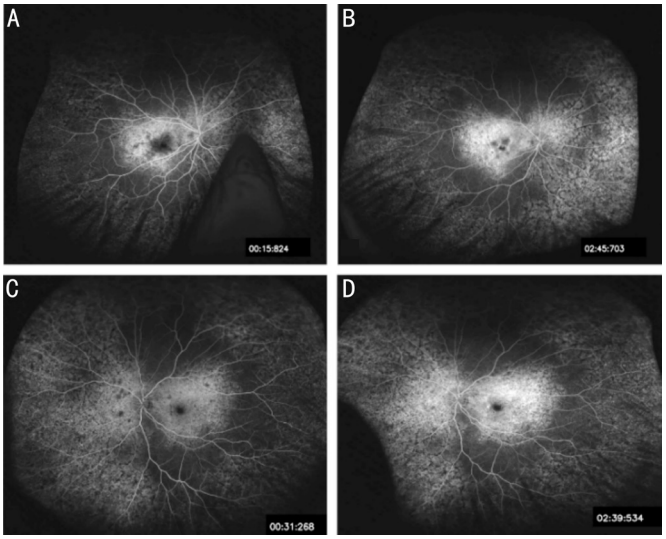

Figure 3 Images of fundus fluorescein angiography (FFA) of the patient FFA images showed widespread hyper-fluorescent window defects with multiple scattered hypo-fluorescent spots in the posterior pole and leakage in the fovea indicating active choroidal neovascularization in both eyes. A-B: Right eye; C-D: Left eye.

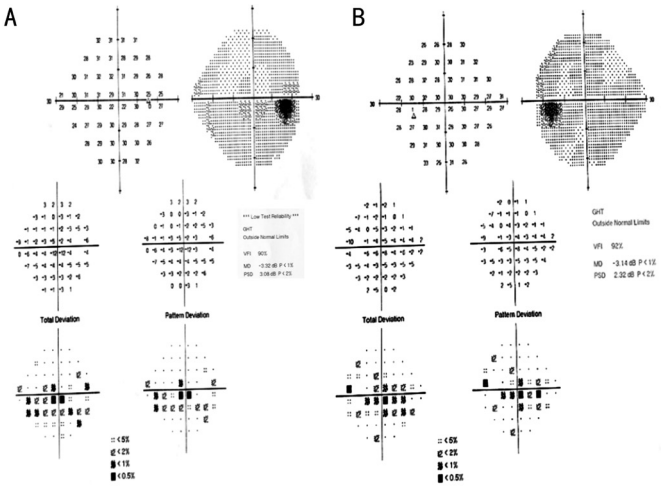

Figure 4 Visual field of the patient showing central scotoma and paracentral scotoma in both eyes A: Right eye; B: Left eye.

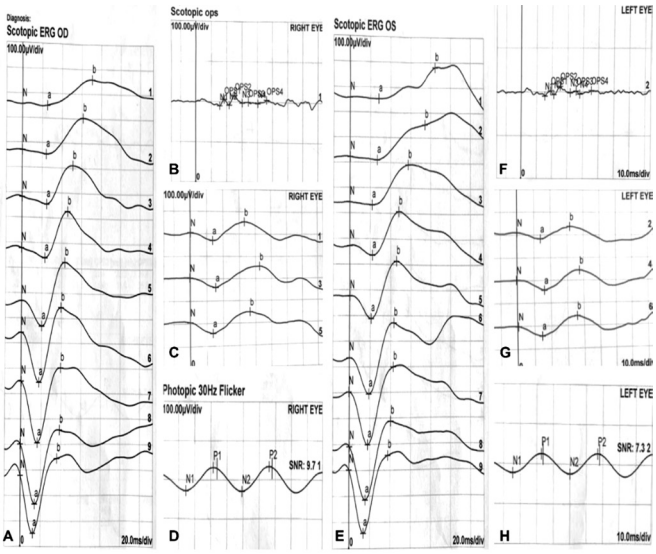

Figure 5 Full-field electroretinography (ERG) of the patient Full-field ERG showed a slightly decreased b-wave amplitude in scotopic ERG. A-D: Right eye; E-H: Left eye.

DISCUSSION

Since the mutation of the *CYP4V2* gene was first reported, the pathogenic mechanism of BCD has been intensively studied, and it has been described as a disorder related to lipid metabolism. The CYP4V2 protein is expressed in almost all kinds of tissues and cells, higher in retinal and RPE cells while relatively lower in corneal cells[5,9]. As an enzyme, the CYP4V2 protein is responsible for the oxidation of substrates during fatty acid metabolism, especially ω-hydroxylation reactions of medium-chain saturated fatty acids. In BCD patients, the conversion of fatty acid (FA) precursors into n-3 polyunsaturated fatty acid (PUFA) is lower than normal, such as the conversion of eicosapentaenoic acid (EPA, 20:5 n-3) and docosahexaenoic acid (DHA, 22:6 n-3) from α-linolenic acid (18:3 n-3)[10]. The eye is rich in DHA, and the photoreceptor cells are the richest in all cells[11]. The membrane disks in the outer segments of photoreceptor cells contain rhodopsin,

phosphatidylcholine, and phosphatidylethanolamine, which converted to DHA and other FA[12]. RPE cells have efficient mechanisms for DHA utilization and recycling, so the cycle of lipids between the outer segments of rods and RPE cells is greatly dependent on the normal functions of RPE cells. This cycle is essential for maintaining normal visual functions so that RPE cells may play an important role in BCD[13-15]. Zhang *et al*[16] have demonstrated that PUFA played an important role in mitochondrial damage inducing RPE degeneration in BCD patients and suggested that adeno-associated virus 2 (AAV2)-mediated gene therapy may be used as the treatment of BCD. Furthermore, some FA metabolites are involved in anti-inflammation, immunoregulation and so on, so that the defections of CYP4V2 protein function may influence the signaling pathway and even influence other aspects[17-18]. Therefore, the mutations of the *CYP4V2* gene may have broad influences, and we still need more detailed studies to clarify the mechanism of BCD.

BCD is characterized by crystals deposit in the retina accompanied by progressive RPE and choriocapillaris atrophy. The progress of BCD was divided into three clinical stages by Yuzawa *et al*[19]. In stage 1, the RPE atrophy is limited to the posterior pole, with the crystals distributed in the posterior pole. In stage 2, the RPE atrophy expands to the equator, and choriocapillaris atrophy appears in the posterior pole. The crystals in the posterior pole may decrease, especially in atrophic areas of the RPE-choriocapillaris complex. In stage 3, RPE-choriocapillaris complex atrophy is extensive, and crystals may be absent. As reported, the crystals are more likely to be located in the relatively healthy retina, especially in areas where RPE is relatively healthy[20-21]. Hence the production of crystals may associate with the abnormal function of RPE. According to this classification, our patient is in stage 2 with typical clinical features.

The OCT images can reveal the location of crystals and the abnormal changes in the choroid and retinal layers. As reported, the crystals are usually located in the RPE-Bruch's membrane complex. They can also be located in the neuroepithelial layer retina, the posterior hyaloid membrane, the space between the retina and vitreum[22-23]. The disorder of the outer retinal layer in BCD, such as the thinning and disruption of RPE, the loss of IZ, and the interruption of EZ, is progressively severe as natural history of the disease. ORTs are considered only appearing in the regions RPE damaged due to the disruption and rearrangement of photoreceptor cells[24-25]. ORTs are more frequently seen in BCD than other degenerative retinal diseases such as age-related macular degeneration (AMD) and RP. The presence of ORTs indicates damaged function of photoreceptor cells and a poor visual prognosis[26-28]. OCT images can also indicate the atrophic change of the choroid. Furthermore, central macular thickness (CMT) measure on OCT can be useful in assessing visual prognosis[29].

AF images help indicate the extent of RPE-choriocapillaris atrophy and photoreceptor cells loss in BCD. In the regions of RPE-choriocapillaris atrophy, the autofluorescence is decreased. The hypo-fluorescence region extends beyond the posterior pole with the disease's progress until there is no fluorescence in the posterior pole in the advanced stage. Hyper-fluorescence spots scatter around the hypo-fluorescence regions in the posterior pole. Though autofluorescence in early stage is usually normal, hyper-fluorescence can sometimes be observed[30].

The early changes of the visual field are mainly central or paracentral scotomas. As the disease progresses, the visual field can be constricted or progress to tubular vision. Electrophysiological tests such as full-field ERG and multifocal ERG can help estimate the severity of degeneration of retinal function. Full-field ERG can reflect dysfunction of rod and cone, varying from normal to amplitudes reduction, even undetectable, depending on disease severity[31]. But sometimes, full-field ERG can remain normal even in the advanced stages of BCD[32]. Multifocal ERG can accurately identify the retina's dysfunctional areas, especially when full-field ERG shows normal results. As the disease progresses, electrooculography (EOG) may show a decrease in the Arden ratio, even earlier than ERG changes[33].

CNV used to be reported as a rare complication of BCD. Actually, the incidence of CNV may be higher than reported in the early stage of BCD, different from other non-syndromic RP[30]. Previously reported cases showed the lesions of CNV in BCD were usually observed in the foveal or parafoveal retina, except in one case of peripapillary CNV[34]. Though the molecular mechanism leading to CNV in BCD has not been elucidated, it does not seem like a direct consequence of the chronic irritation of Bruch's membrane by the intraretinal crystals, or the lesions will scatter throughout the whole posterior pole. Researchers have demonstrated that CNV in BCD may be attributed to the abnormalities of photoreceptor outer segment RPE interface at the fovea and parafovea[35]. Intravitreal injection of anti-VEGF agents such as ranibizumab has been shown to be effective in treating CNV as a complication of BCD[36-37]. Moreover, OCTA is a new way to monitor choroidal blood flow changes in BCD, revealing the decrease of choroidal blood flow and abnormal angiogenesis in the choroid[38]. In addition, Xu *et al*[39] reported that the deficit of choroidal perfusion impaired in BCD may be more pathologic than the deficit retinal blood perfusion.

Up to now, dozens of pathogenic mutations of *CYP4V2* have been reported. Among the mutations, the most common pathogenic mutation in BCD is c.802-8del17bp/insGC (IVS6-

8del17bp/insGC), a deletion-insertion (delins/indel) mutation at the junction of intron 6 and exon 7[40]. Though researchers have not found clear genotype-phenotype correlations in patients with BCD, some studies have suggested that the disease phenotype of homozygous or heterozygous c.802-8del17bp/insGC mutation seemed to be more severe, as a result of exon 7 skipped and the expression of CYP4V2 protein truncated[29,41]. Similarly, deletion mutations may lead to a more severe disease phenotype, compared with milder substitution mutation[22,42]. Besides, the variability of BCD phenotype suggests that many factors affecting lipid metabolism may affect the phenotype and disease progression of BCD, such as diet, inflammation, and so much more[43]. We found three heterozygous mutations in the *CYP4V2* gene in this study. The c.802_807del and c.810delT are deletion mutations, and the c.1388G>A is a substitution mutation that has never been reported before. The c.810delT has been reported by Jiao *et al*[10]. They reported that the mutation leads to p.A270fs*5, a frameshift mutation of amino acid 270, and a premature translation stop. Moreover, its mRNA is predicted to undergo nonsense-mediated decay (NMD). It is predicted to be "Disease Causing" with a probability value of 1 based on Mutation Taster. The c.802_807del reported by Wang *et al*[8] results in p.V268_I269del (deletion of amino acids Valine and Isoleucine at 268 to 269). But the prediction of this mutation is "Polymorphism" with a probability value of 0.940042106165059 based on Mutation Taster. The novel mutation c.1388G>A results in an amino acid substitution from Glycine to Asparticacid, predicted to be "Disease Causing" with a probability value of 0.999999999999894 based on Mutation Taster. It is predicted to cause amino acid sequence changed, protein features affected, and splice site changes. It is also predicted to be "Probably Damaging" with a score of 1.000 (sensitivity: 0.00; specificity: 1.00) based on PolyPhen-2, and "Deleterious" with a score of -6.711 based on Provean. But whether this novel mutation was related to a complication of CNV needs further study. Considered the limit of prediction tools, the exact mechanism remains to be clarified.

In conclusion, we reported c.1388G>A as a novel mutation in the *CYP4V2* gene and predicted the damaging of the novel mutation using bioinformatics tools. Our findings expand the mutation spectrum of the *CYP4V2* gene in BCD.

ACKNOWLEDGEMENTS

Foundations: Supported by National Key R&D Program of China (No.2020YFC2008200); Capital Clinical Diagnosis and Treatment Technology Research and Demonstration Application Project of China (No.Z191100006619029).

Conflicts of Interest: Han XY, None; **Zhang LQ,** None; **Tang JY,** None; **Huang LZ,** None; **Tang R,** None; **Qu JF,** None.

REFERENCES

1 Tsang SH, Sharma T. Inborn errors of metabolism: Bietti crystalline dystrophy. *Adv Exp Med Biol* 2018;1085:193-195.

2 Garli M, Kurna SA. A case of Bietti crystalline dystrophy with clinical, electrophysiological, and imaging findings. *North Clin Istanb* 2021;8(5):521-524.

3 da Palma MM, Motta FL, Salles MV, Texeira CHM, Gomes AV, Casaroli-Marano R, Sallum JMF. Expanding the phenotypic and genotypic spectrum of Bietti crystalline dystrophy. *Genes* (*Basel*) 2021;12(5):713.

4 Hu DN. Genetic aspects of retinitis pigmentosa in China. *Am J Med Genet* 1982;12(1):51-56.

5 Li A, Jiao X, Munier FL, Schorderet DF, Yao W, Iwata F, Hayakawa M, Kanai A, Shy Chen M, Alan Lewis R, Heckenlively J, Weleber RG, Traboulsi EI, Zhang Q, Xiao X, Kaiser-Kupfer M, Sergeev YV, Hejtmancik JF. Bietti crystalline corneoretinal dystrophy is caused by mutations in the novel gene CYP4V2. *Am J Hum Genet* 2004;74(5):817-826.

6 Nakano M, Kelly EJ, Rettie AE. Expression and characterization of CYP4V2 as a fatty acid omega-hydroxylase. *Drug Metab Dispos* 2009;37(11):2119-2122.

7 Hata M, Ikeda HO, Iwai S, Iida Y, Gotoh N, Asaka I, Ikeda K, Isobe Y, Hori A, Nakagawa S, Yamato S, Arita M, Yoshimura N, Tsujikawa A. Reduction of lipid accumulation rescues Bietti's crystalline dystrophy phenotypes. *Proc Natl Acad Sci U S A* 2018;115(15):3936-3941.

8 Wang W, Chen W, Bai X, Chen L. Multimodal imaging features and genetic findings in Bietti crystalline dystrophy. *BMC Ophthalmol* 2020;20(1):331.

9 García-García GP, Martínez-Rubio M, Moya-Moya MA, Pérez-Santonja JJ, Escribano J. Current perspectives in Bietti crystalline dystrophy. *Clin Ophthalmol* 2019;13:1379-1399.

10 Jiao X, Li A, Jin ZB, Wang X, Iannaccone A, Traboulsi EI, Gorin MB, Simonelli F, Hejtmancik JF. Identification and population history of CYP4V2 mutations in patients with Bietti crystalline corneoretinal dystrophy. *Eur J Hum Genet* 2017;25(4):461-471.

11 Miyagishima KJ, Sharma R, Nimmagadda M, Clore-Gronenborn K, Qureshy Z, Ortolan D, Bose D, Farnoodian M, Zhang C, Fausey A, Sergeev YV, Abu-Asab M, Jun B, Do KV, Kautzman Guerin MA, Calandria J, George A, Guan B, Wan Q, Sharp RC, Cukras C, Sieving PA, Hufnagel RB, Bazan NG, Boesze-Battaglia K, Miller S, Bharti K. AMPK modulation ameliorates dominant disease phenotypes of CTRP5 variant in retinal degeneration. *Commun Biol* 2021;4(1):1360.

12 Anderson RE. Lipids of ocular tissues. IV. A comparison of the phospholipids from the retina of six mammalian species. *Exp Eye Res* 1970;10(2):339-344.

13 Giusto NM, Pasquaré SJ, Salvador GA, Castagnet PI, Roque ME, Ilincheta de Boschero MG. Lipid metabolism in vertebrate retinal rod outer segments. *Prog Lipid Res* 2000;39(4):315-391.

14 Gordon WC, Bazan NG. Visualization of [3H]docosahexaenoic acid trafficking through photoreceptors and retinal pigment epithelium by electron microscopic autoradiography. *Invest Ophthalmol Vis Sci* 1993;34(8):2402-2411.

15 Bazan NG. Cell survival matters: docosahexaenoic acid signaling, neuroprotection and photoreceptors. *Trends Neurosci* 2006;29(5):263-271.

16 Zhang Z, Yan B, Gao F, Li Q, Meng XH, Chen PK, Zhou L, Deng W, Li C, Xu WY, Han S, Feng H, Li YP, Chen JH, Yin ZQ, Liao C, Tse HF, Xu AM, Lian QZ. PSCs reveal PUFA-provoked mitochondrial stress as a central node potentiating RPE degeneration in Bietti's crystalline dystrophy. *Mol Ther* 2020;28(12):2642-2661.

17 Reyes-Reveles J, Dhingra A, Alexander D, Bragin A, Philp NJ, Boesze-Battaglia K. Phagocytosis-dependent ketogenesis in retinal pigment epithelium. *J Biol Chem* 2017;292(19):8038-8047.

18 Ni KD, Liu JY. The functions of cytochrome P450 ω-hydroxylases and the associated eicosanoids in inflammation-related diseases. *Front Pharmacol* 2021;12:716801.

19 Yuzawa M, Mae Y, Matsui M. Bietti's crystalline retinopathy. *Ophthalmic Paediatr Genet* 1986;7(1):9-20.

20 Halford S, Liew G, Mackay DS, Sergouniotis PI, Holt R, Broadgate S, Volpi EV, Ocaka L, Robson AG, Holder GE, Moore AT, Michaelides M, Webster AR. Detailed phenotypic and genotypic characterization of Bietti crystalline dystrophy. *Ophthalmology* 2014;121(6):1174-1184.

21 Gocho K, Kameya S, Akeo K, Kikuchi S, Usui A, Yamaki K, Hayashi T, Tsuneoka H, Mizota A, Takahashi H. High-resolution imaging of patients with Bietti crystalline dystrophy with CYP4V2 mutation. *J Ophthalmol* 2014;2014:283603.

22 Pennesi ME, Weleber RG. High-resolution optical coherence tomography shows new aspects of Bietti crystalline retinopathy. *Retina* 2010;30(3):531-532.

23 Toto L, Carpineto P, Parodi MB, di Antonio L, Mastropasqua A, Mastropasqua L. Spectral domain optical coherence tomography and *in vivo* confocal microscopy imaging of a case of Bietti's crystalline dystrophy. *Clin Exp Optom* 2013;96(1):39-45.

24 Huang XL, Song YP, Ding Q, Chen X, Hong L. Evaluation of outer retinal tubulations in diabetic macular edema underwent anti-VEGF treatment. *Int J Ophthalmol* 2019;12(3):442-450.

25 Janse van Rensburg E, Ryu CL, Rampakakis E, Vila N, Chan EW, Chen JC. Outer retinal tubulation may result from fibrosed type 2 neovascularization: clinical observations and model of pathogenesis. *Retina* 2021;41(9):1930-1939.

26 Kovacs A, Kiss T, Rarosi F, Somfai GM, Facsko A, Degi R. The effect of ranibizumab and aflibercept treatment on the prevalence of outer retinal tubulation and its influence on retreatment in neovascular age-related macular degeneration. *BMC Ophthalmol* 2018;18(1):298.

27 Arrigo A, Aragona E, Battaglia O, Saladino A, Amato A, Borghesan F, Pina A, Calcagno F, Hassan Farah R, Bandello F, Battaglia Parodi M. Outer retinal tubulation formation and clinical course of advanced age-related macular degeneration. *Sci Rep* 2021;11(1):14735.

28 Dolz-Marco R, Litts KM, Tan ACS, Freund KB, Curcio CA. The evolution of outer retinal tubulation, a neurodegeneration and gliosis prominent in macular diseases. *Ophthalmology* 2017;124(9):1353-1367.

29 Lai TY, Ng TK, Tam PO, Yam GH, Ngai JW, Chan WM, Liu DT, Lam DS, Pang CP. Genotype phenotype analysis of Bietti's crystalline dystrophy in patients with CYP4V2 mutations. *Invest Ophthalmol Vis Sci* 2007;48(11):5212-5220.

30 Pole C, Ameri H. Fundus autofluorescence and clinical applications. *J Ophthalmic Vis Res* 2021;16(3):432-461.

31 Usui T, Tanimoto N, Takagi M, Hasegawa S, Abe H. Rod and cone a-waves in three cases of Bietti crystalline chorioretinal dystrophy. *Am J Ophthalmol* 2001;132(3):395-402.

32 Rossi S, Testa F, Li A, Yaylacioğlu F, Gesualdo C, Hejtmancik JF, Simonelli F. Clinical and genetic features in Italian Bietti crystalline dystrophy patients. *Br J Ophthalmol* 2013;97(2):174-179.

33 Haddad NM, Waked N, Bejjani R, Khoueir Z, Chouery E, Corbani S, Mégarbané A. Clinical and molecular findings in three Lebanese families with Bietti crystalline dystrophy: report on a novel mutation. *Mol Vis* 2012;18:1182-1188.

34 Kobat SG, Gul FC, Yusufoglu E. Bietti crystalline dystrophy and choroidal neovascularization in childhood. *Int J Ophthalmol* 2019;12(9):1514-1516.

35 Fuerst NM, Serrano L, Han G, Morgan JI, Maguire AM, Leroy BP, Kim BJ, Aleman TS. Detailed functional and structural phenotype of Bietti crystalline dystrophy associated with mutations in CYP4V2 complicated by choroidal neovascularization. *Ophthalmic Genet* 2016;37(4):445-452.

36 Le Tien V, Atmani K, Querques G, Massamba N, Souied EH. Ranibizumab for subfoveal choroidal neovascularization in Bietti crystalline retinopathy. *Eye* (*Lond*) 2010;24(11):1728-1729.

37 Nachiappan K, Krishnan T, Madhavan J. Ranibizumab for choroidal neovascular membrane in a rare case of Bietti's crystalline dystrophy: a case report. *Indian J Ophthalmol* 2012;60(3):207-209.

38 Miyata M, Oishi A, Hasegawa T, Ishihara K, Oishi M, Ogino K, Sugahara M, Hirashima T, Hata M, Yoshikawa M, Tsujikawa A. Choriocapillaris flow deficit in Bietti crystalline dystrophy detected using optical coherence tomography angiography. *Br J Ophthalmol* 2018;102(9):1208-1212.

39 Xu Y, Qin Z, Wu N, Zhao T, Gu P, Ren B, Li L, Meng X, Liu Y. Retinal and choroidal blood perfusion in patients with Bietti crystalline dystrophy. *Retina* 2021;41(11):2351-2360.

40 Meng XH, Guo H, Xu HW, Li QY, Jin X, Bai Y, Li SY, Yin ZQ. Identification of novel *CYP4V2* gene mutations in 92 Chinese families with Bietti's crystalline corneoretinal dystrophy. *Mol Vis* 2014;20:1806-1814.

41 Bai Z, Xie Y, Liu L, Shao J, Liu Y, Kong X. Genetic investigation of 211 Chinese families expands the mutational and phenotypical spectra of hereditary retinopathy genes through targeted sequencing technology. *BMC Med Genomics* 2021;14(1):92.

42 Ng DS, Lai TY, Ng TK, Pang CP. Genetics of Bietti crystalline dystrophy. *Asia Pac J Ophthalmol (Phila)* 2016;5(4):245-252.

43 Lockhart CM, Smith TB, Yang P, Naidu M, Rettie AE, Nath A, Weleber R, Kelly EJ. Longitudinal characterisation of function and structure of Bietti crystalline dystrophy: report on a novel homozygous mutation in CYP4V2. *Br J Ophthalmol* 2018;102(2):187-194.